Electron Cryomicroscopy of E. coli Reveals Filament Bundles Involved in Plasmid DNA Segregation

Jeanne Salje, *et al.*

Science **323**, 509 (2009);
DOI: 10.1126/science.1164346

8. Materials and methods are available as supporting material on *Science* Online.
9. S. Srinivas *et al.*, *BMC Dev. Biol.* **1**, 4 (2001).
10. A. L. Marzo *et al.*, *Nat. Immunol.* **6**, 793 (2005).
11. J. Jacob, D. Baltimore, *Nature* **399**, 593 (1999).
12. R. D. Hanson, G. M. Sclar, O. Kanagawa, T. J. Ley, *J. Biol. Chem.* **266**, 24433 (1991).
13. M. R. Jenkins *et al.*, *J. Immunol.* **181**, 3818 (2008).
14. M. A. Williams, A. J. Tyznik, M. J. Bevan, *Nature* **441**, 890 (2006).
15. L. E. Harrington, K. M. Janowski, J. R. Oliver, A. J. Zajac, C. T. Weaver, *Nature* **452**, 356 (2008).
16. The authors thank D. Winton for ROSA26EYFP mice, B. Crombrugghe for the CreER^{T2} construct, G. Eberl for the recombineering shuttle vector, and P. Digard and E. Hutchinson for help with viruses. This work was funded by the Wellcome Trust.

Supporting Online Material
www.sciencemag.org/cgi/content/full/323/5913/505/DC1
Materials and Methods
Figs. S1 to S3
Table S1
References

6 October 2008; accepted 1 December 2008
10.1126/science.1166831

Electron Cryomicroscopy of *E. coli* Reveals Filament Bundles Involved in Plasmid DNA Segregation

Jeanne Salje,*† Benoît Zuber, Jan Löwe

Bipolar elongation of filaments of the bacterial actin homolog ParM drives movement of newly replicated plasmid DNA to opposite poles of a bacterial cell. We used a combination of vitreous sectioning and electron cryotomography to study this DNA partitioning system directly in native, frozen cells. The diffraction patterns from overexpressed ParM bundles in electron cryotomographic reconstructions were used to unambiguously identify ParM filaments in *Escherichia coli* cells. Using a low–copy number plasmid encoding components required for partitioning, we observed small bundles of three to five intracellular ParM filaments that were situated close to the edge of the nucleoid. We propose that this may indicate the capture of plasmid DNA within the periphery of this loosely defined, chromosome-containing region.

One of the simplest known mechanisms by which newly replicated DNA molecules are moved apart is encoded by the bacterial low–copy number plasmid R1. This type II plasmid partitioning system includes three components that are both necessary and sufficient to confer genetic stability and are encoded in a tight gene cluster (*1*). ParM is an actin-like adenosine triphosphatase (ATPase) protein that forms double-helical filaments (*2*–*4*) and exhibits dynamic instability from both ends in the presence of ATP (*5*). Upon addition of both the small DNA-binding protein ParR and the centromere-like DNA region, *parC*, a ParR*C* protein-DNA complex caps and stabilizes both ends of the ParM filament (*6*–*8*). Thus stabilized, the ParM filament elongates at both ends and drives the plasmid-attached ParR*C* complexes to opposite poles of the bacterial cell. This system has been extensively studied both in cells using light microscopy (*9*–*11*) and in vitro (*5*, *6*), and here we turn to a direct characterization of ParMR*C*-driven DNA segregation in situ using vitreous sectioning (*12*) and electron cryotomography.

First, we set about characterizing ParM filaments directly in *E*scherichia *coli* cells that had been immobilized in a near-to-native vitreous state by high-pressure freezing (*13*). ParM was overexpressed to very high concentrations in the absence of ParR or *parC*. ParM filaments form spontaneously at these high concentrations. Images of cryosections revealed that these cells contained a large volume of tightly packed bundles of filaments (Fig. 1A and fig. S1A). This packing is probably due to the crowded environment of the cell. A small amount of crowding agent is sufficient to induce bundling of purified ParM filaments (Fig. 1, B and C) (*14*). Unlike actin, no additional proteins that induce bundling by cross-linking along the filaments of ParM are known or required.

To verify the identity of the bundles of filaments as ParM protein, we compared the diffraction patterns from electron cryomicrographs of in vitro bundles with those extracted from in situ electron cryotomography reconstructions. The resulting lateral diffraction spacing corresponds to packing of the roughly 80 Å thick filaments and was determined to be 83 Å in the tomogram slice (Fig. 1, D and E) and smeared between 63 and 83 Å for the in vitro bundles (Fig. 1, E and F). This smear relates to the fact that in vitro bundles were several filaments thick, producing additional, smaller interfilament repeats in the diffraction pattern. The longitudinal repeat of filamentous ParM was measured to be 53 Å in the in vitro bundles (Fig. 1E), agreeing with previous measurements on single filaments (*2*, *4*). We were able to measure the longitudinal repeat in tomographic slices, and this ranged from 41 to 53 Å, depending on the angle of rotation. The upper value confirmed the identity of these filaments. Bundles of filaments persisted in the presence of the MreB-depolymerizing drug A22 (fig. S1B), ruling out the possibility that these filaments were composed of the chromosomally encoded bacterial actin MreB.

As a comparison, we performed electron cryotomography on whole, intact plunge-frozen cells containing bundles of ParM (Fig. 1G). These cells expressed an ATPase-deficient mutant form of ParM [Asp^{170} → Ala^{170} (D170A)] (*11*), which is unable to depolymerize, leading to strings of cells with blocked septa. Even here the sample was too thick to achieve resolutions comparable to those obtained using thin cryosections, and the longitudinal repeat in the diffraction pattern could not be detected (compare Fig. 1, E and G).

Having identified ParM filaments directly in cryo-immobilized cells, we next turned to studying intracellular ParM filaments that are actively involved in segregating plasmid DNA. We used three different systems, each moving closer to the situation of the original R1 low-copy plasmid system (Fig. 2A). The first system was T7-driven ParM overexpression (see above). Next, we put three copies of the ParMR*C* cluster on a high–copy number plasmid (pBR322 replicon). Finally, a low–copy number R1-derived plasmid stabilized by a single copy of the ParMR*C* partitioning complex was used (pKG491) (*1*, *15*). A marked decrease in ParM levels was observed, moving from the overexpression system through the high–copy number plasmid to the low–copy number R1-derived plasmid (Fig. 2A). Cross sections through frozen cells overexpressing ParM protein clearly revealed tightly packed bundles of ParM (Fig. 2B, left, and fig. S1A). These images told us that ParM filaments would be best recognized in cross sections through the filaments (Fig. 2C). Cells carrying the ParMR*C*-containing high–copy number plasmid contained a combination of small bundles and single filaments within a single cell (Fig. 2B, middle, and fig. S2, A to C). Moving to even lower ParM concentrations using cells carrying the low–copy number R1 plasmid pKG491, we anticipated that observing filaments would be an extremely rare event. Previous studies have shown that pole-to-pole filaments of ParM can be observed in only ~40% of cells, with the others localizing in discrete clusters or diffuse throughout the cell (*11*). Furthermore, our ParM overexpression experiments told us that filaments could only be confidently recognized in those sections where the filament is exactly perpendicular to the imaging plane. Given that cells are frozen and sectioned in a semi-random orientation, we therefore imaged 300 to 400 cells.

Medical Research Council (MRC) Laboratory of Molecular Biology, Hills Road, Cambridge CB2 0QH, UK.

*To whom correspondence should be addressed. E-mail: jsalje@mrc-lmb.cam.ac.uk
†Present address: Kyoto University, Department of Biophysics, Faculty of Science, Oiwake Kitashirakawa, Sakyo-Ku, Kyoto 606-8502, Japan.

In spite of these difficulties, we were able to identify small bundles of three to five filaments in cross sections of cells harboring the R1-derived low-copy plasmid (Fig. 2, B, right, and D). All filament bundles that we identified are shown in fig. S3, A to G. Similar structures were never observed in 385 images of plasmid-free cells (fig. S4, A to F). The packing of the bundles matched that observed in both the overexpression and high–copy number systems (Fig. 2B). We cannot formally prove that the ParM bundles we observed were actively segregating attached plasmids and had not formed spontaneously because we cannot co-label the plasmid DNA and fully trace the filament through the cell. However, we find it highly probable that these bundles were in the process of segregating or anchoring plasmids for the following reasons. First, the high–copy number plasmid experiment showed that not all filaments bundle spontaneously at these low ParM concentrations (Fig. 2B and fig. S2, A to C). Thus, a plasmid-related process, such as clustering, must have induced the bundles we observed in the R1 derivative. Second, ParM filaments only form in these cells in the presence of both ParR and *parC* (*11*), and plasmids localize to the ends of ParM filaments (*10*). Third, the plasmid copy number (4 to 6) (*16*) closely matches the number of filaments observed in our bundles (3 to 5), strongly supporting the current model for ParMR*C* DNA segregation (*8*).

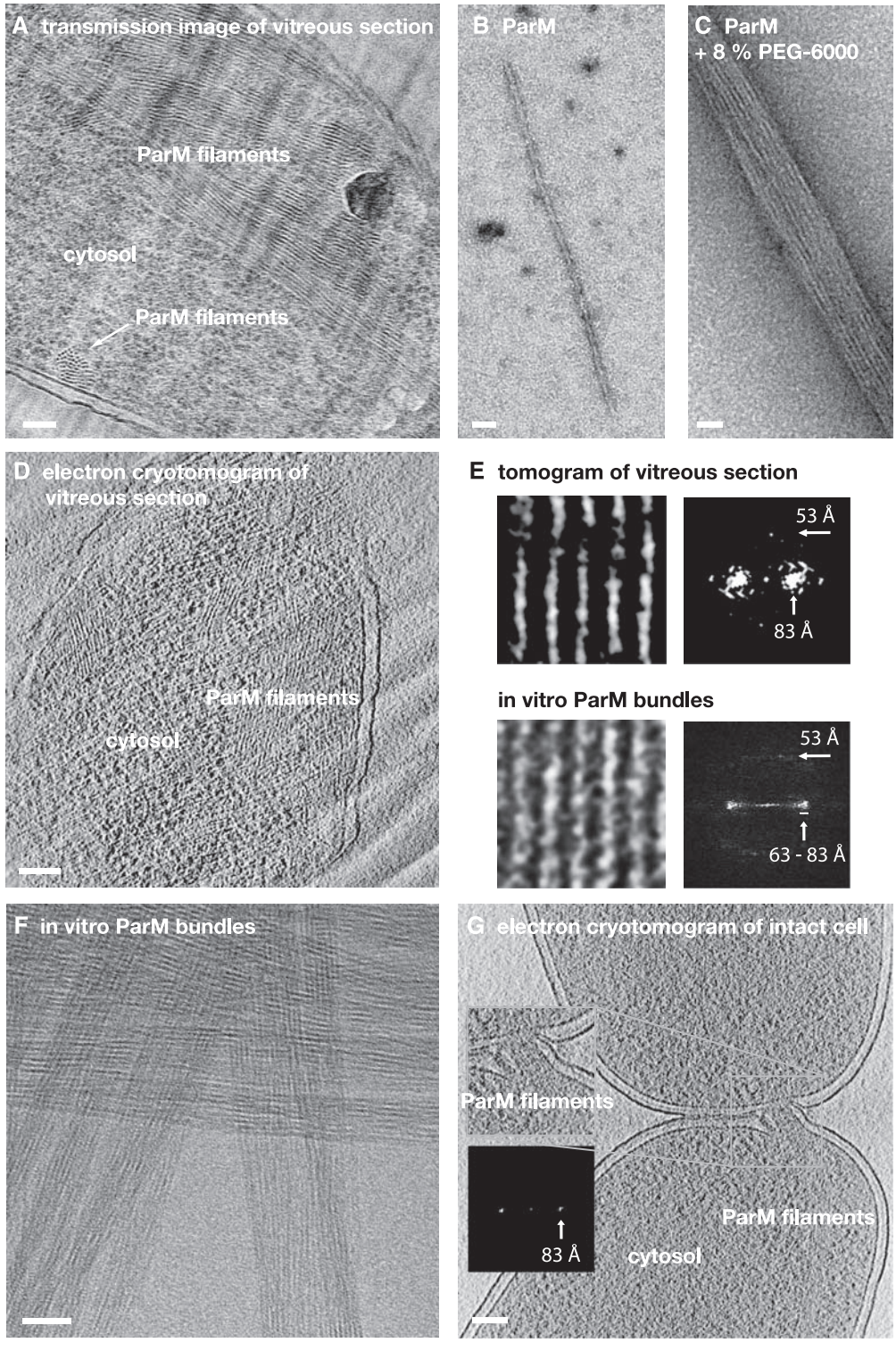

Fig. 1. Direct observation of bundles of ParM filaments in frozen *E. coli* cells. (**A**) Transmission image of a vitreous cryosection of a cell containing overexpressed ParM filaments. (**B** and **C**) Negatively stained in vitro ParM filaments in the presence (C) and absence (B) of crowding agent (8% PEG-6000). (**D**) Slice through a three-dimensional (3D) tomographic reconstruction of a vitreous cryosection of a cell containing overexpressed ParM filaments. (**E**) Diffraction patterns from a 3D tomographic reconstruction slice [top, as shown in (D)] or in vitro bundles of ParM [bottom, as shown in (F)]. (**F**) Electron micrograph of bundles of frozen in vitro ParM filaments formed in the presence of 8% PEG-6000. (**G**) Slice through a 3D tomographic reconstruction of a whole, intact plunge-frozen cell containing $D^{170}A$ (ATPase-defective) ParM filaments. The diffraction pattern from a small bundle extracted from the tomogram is shown. Scale bars are 100 nm [(A), (D), (E), and (G)] or 20 nm [(B) and (C)].

How are the filaments bundled in the cell? One possible explanation is that plasmids can be linked via the oligomeric ParR*C* complexes (*17*), and these linked complexes can bring together the ends of two ParM filaments (*8*). This may lead to bundling, as supported by the observation that covalently linked clusters of ParR–*parC* are sufficient to induce ParM bundling in vitro (*18*).

We next turned our attention to the subcellular localization of plasmid-segregating ParM bundles. Fluorescently labeled ParM from low–copy number plasmids forms curved pole-to-pole filaments running close to the edge of the bacterial cell (*9*–*11*) (Fig. 3E). Because of the small size of the cells (~0.8 to 1 μm thick), it has so far been impossible to distinguish whether the filaments are attached to the inner surface of the cell membrane or run through the cytosol, or where they lie relative to the bacterial nucleoid. Direct visualization of ParM bundles in cells using vitreous sectioning offers the advantage that subcellular localization can be defined with high precision and that the nucleoid can easily be recognized as a region of low contrast (*19*).

We found that bundles of ParM filaments segregating the low–copy number R1 derivative were localized near the edge of the bacterial nucleoid (Fig. 3A and fig. S5). Out of seven good images of bundles, five were localized near the edge of the nucleoid, and the nucleoid was absent in the other two sections. This positioning suggests that the plasmids at the ends of the filaments are loosely captured within the nucleoid DNA region, and this gives the first high-resolution insight into intracellular plasmid localization (Fig. 3D). The prediction that these R1-derived ParM bundles point to plasmid localization within or near the nucleoid is supported by the observation that ParM filaments in cells carrying ParMR*C*-containing high–copy number plasmids also cluster both in and around the nucleoid (Fig. 3B and fig. S2, A to C).

Our observations that plasmid-segregating ParM filaments are associated with the nucleoid and the ensuing prediction that plasmids are anchored therein immediately leads us to two further questions. First, where exactly do the ends of ParM filaments and the associated newly segregated plasmids lie in the cell? This relates to the question of how close the nucleoid extends into the poles of a bacterium. With the use of immunofluorescence microscopy, we found that ParM filaments extend close to the poles of the cells (Fig. 3E) in line with earlier experiments (*10*, *20*, *21*), but the resolution of these images is limited. The second question relates to the cause and nature of plasmid capture within or near the nucleoid. This association must be only weakly maintained because elongating ParM filaments push plasmids through the cell at a rate of 3.1 μm/min (*9*).

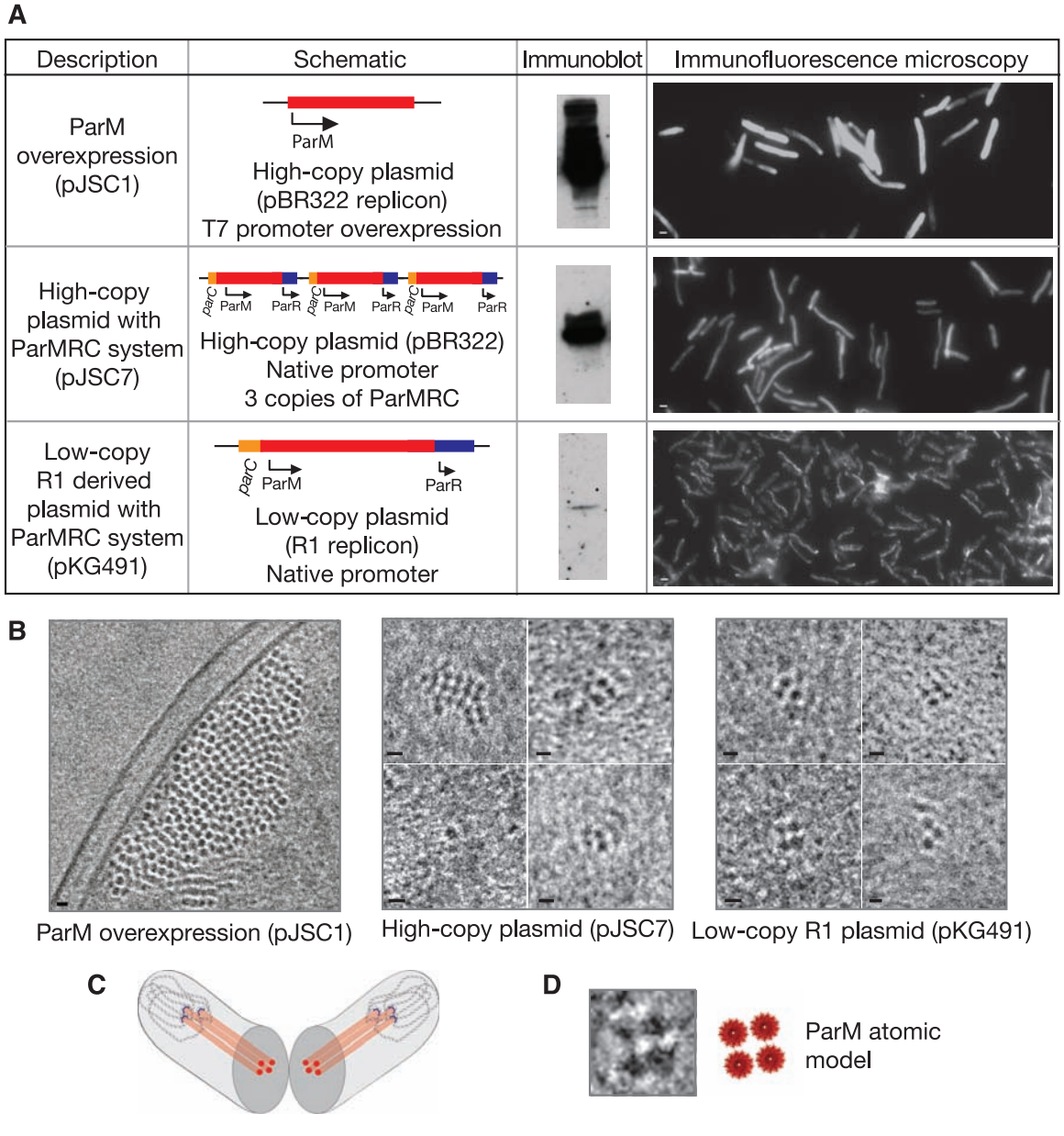

Fig. 2. Small bundles of ParM filaments are involved in plasmid-DNA segregation. (**A**) Three different systems used to study ParM filaments in vitreous sections. (**B**) Vitreous cryosections of cells described in (A) showing end-on views of ParM filaments. (**C**) The plane of imaging is perpendicular to the filaments to achieve high contrast and recognize the characteristic packing. (**D**) To-scale atomic interpretation of the ParM bundles observed in (B). Scale bars are 1 μm (A) or 10 nm (B).

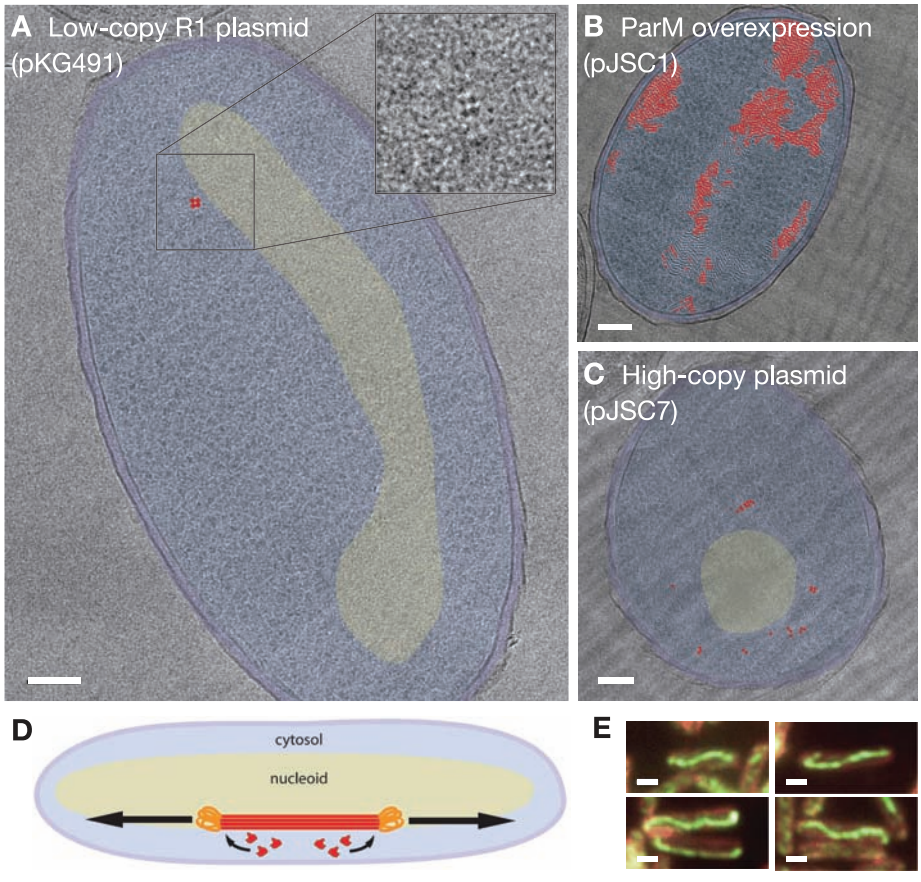

Fig. 3. Bundles of ParM filaments involved in R1 plasmid DNA segregation lie at the periphery of the nucleoid and may indicate plasmid capture therein. (**A** to **C**) Vitreous cryosections of cells carrying (A) pKG491 (low-copy), (B) pJSC1 (overexpression), and (C) pJSC7 (high-copy) plasmids. Dark blue, cell wall; light blue, cytosol; yellow, nucleoid; red, ParM filaments. Raw images are given in fig. S3, A to G. (**D**) A model for ParM-driven R1 plasmid DNA segregation. (**E**) Immunofluorescence microscopy showing ParM in cells carrying pKG491. ParM, green; membranes, red. Scale bars are 100 nm [(A) to (C)] or 1 μm (E).

Such plasmid capture within the nucleoid may be achieved through association with host-encoded replication/transcription machinery or by linkage with bacterial condensins (*21*).

References and Notes

1. K. Gerdes, S. Molin, *J. Mol. Biol.* **190**, 269 (1986).
2. A. Orlova *et al.*, *Nat. Struct. Mol. Biol.* **14**, 921 (2007).
3. D. Popp *et al.*, *EMBO J.* **27**, 570 (2008).
4. F. van den Ent, J. Møller-Jensen, L. A. Amos, K. Gerdes, J. Löwe, *EMBO J.* **21**, 6935 (2002).
5. E. C. Garner, C. S. Campbell, R. D. Mullins, *Science* **306**, 1021 (2004).
6. E. C. Garner, C. S. Campbell, D. B. Weibel, R. D. Mullins, *Science* **315**, 1270 (2007).
7. R. B. Jensen, K. Gerdes, *J. Mol. Biol.* **269**, 505 (1997).
8. J. Salje, J. Löwe, *EMBO J.* **27**, 2230 (2008).
9. C. S. Campbell, R. D. Mullins, *J. Cell Biol.* **179**, 1059 (2007).
10. J. Møller-Jensen *et al.*, *Mol. Cell* **12**, 1477 (2003).
11. J. Møller-Jensen, R. B. Jensen, J. Löwe, K. Gerdes, *EMBO J.* **21**, 3119 (2002).
12. A. Al-Amoudi *et al.*, *EMBO J.* **23**, 3583 (2004).
13. Materials and methods are available as supporting material on *Science* Online.
14. D. Popp *et al.*, *Biochem. Biophys. Res. Commun.* **353**, 109 (2007).
15. M. Dam, K. Gerdes, *J. Mol. Biol.* **236**, 1289 (1994).
16. K. Nordström, S. Molin, H. Aagaard-Hansen, *Plasmid* **4**, 332 (1980).
17. R. B. Jensen, R. Lurz, K. Gerdes, *Proc. Natl. Acad. Sci. U.S.A.* **95**, 8550 (1998).
18. C. L. Choi, S. A. Claridge, E. C. Garner, A. P. Alivisatos, R. D. Mullins, *J. Biol. Chem.* **283**, 28081 (2008).
19. M. Eltsov, B. Zuber, *J. Struct. Biol.* **156**, 246 (2006).
20. G. Ebersbach, D. J. Sherratt, K. Gerdes, *Mol. Microbiol.* **56**, 1430 (2005).
21. T. Weitao, S. Dasgupta, K. Nordström, *Mol. Microbiol.* **38**, 392 (2000).

22. We thank K. Gerdes (Newcastle, UK) and J. Møller-Jensen (Odense, Denmark) for kindly supplying plasmids and strains and W. Kühlbrandt and D. Mills (Frankfurt, Germany) for generously allowing us the use of their microscope. J.S. is supported by MRC and Leverhulme Trust studentships, and B.Z. is supported by a European Molecular Biology Organization long-term fellowship. J.S. performed all experiments and their analysis except the initial cryo-sectioning that was done with B.Z.

Supporting Online Material

www.sciencemag.org/cgi/content/full/1164346/DC1
Materials and Methods
Figs. S1 to S5
References

7 August 2008; accepted 24 November 2008
Published online 18 December 2008;
10.1126/science.1164346
Include this information when citing this paper.

Alternative Zippering as an On-Off Switch for SNARE-Mediated Fusion

Claudio G. Giraudo,[1]*† Alejandro Garcia-Diaz,[1]† William S. Eng,[1,2] Yuhang Chen,[2] Wayne A. Hendrickson,[2] Thomas J. Melia,[1]† James E. Rothman[1]*†

Membrane fusion between vesicles and target membranes involves the zippering of a four-helix bundle generated by constituent helices derived from target– and vesicle–soluble *N*-ethylmaleimide–sensitive factor attachment protein receptors (SNAREs). In neurons, the protein complexin clamps otherwise spontaneous fusion by SNARE proteins, allowing neurotransmitters and other mediators to be secreted when and where they are needed as this clamp is released. The membrane-proximal accessory helix of complexin is necessary for clamping, but its mechanism of action is unknown. Here, we present experiments using a reconstituted fusion system that suggest a simple model in which the complexin accessory helix forms an alternative four-helix bundle with the target-SNARE near the membrane, preventing the vesicle-SNARE from completing its zippering.

Intracellular membrane fusion is catalyzed by the assembly of SNARE complexes between membranes, forcing their bilayers together (*1*, *2*). Because SNARE complex assembly is strongly favored energetically (*3*), fusion will occur spontaneously in the absence of additional proteins that may be provided to prevent this from happening. However, in synaptic transmission and hormone release, fusion does not occur until calcium enters the presynaptic cytoplasm when the action potential terminates at the nerve ending. Although synaptic vesicles are primed and ready with their SNAREs largely zippered (*4*), they are unable to complete fusion without calcium (*5*–*7*). Complexin (CPX) can function as a clamp (*8*) by binding the helical bundle of

[1]Department of Physiology and Cellular Biophysics, Columbia University, College of Physicians and Surgeons, 1150 Saint Nicholas Avenue, Russ Berrie Building, Room 520, New York, NY 10032, USA. [2]Department of Biochemistry and Molecular Biophysics, Columbia University, and Howard Hughes Medical Institute, New York, NY 10032, USA.

*To whom correspondence should be addressed. E-mail: james.rothman@yale.edu (J.E.R.); claudio.giraudo@yale.edu (C.G.G.)

†Present address: Department of Cell Biology, School of Medicine, Yale University, 333 Cedar Street, New Haven, CT 06520, USA.